

Showcasing research from Associate Professor Elijah Thimsen's laboratory, Department of Energy, Environmental & Chemical Engineering, Washington University in St. Louis, St. Louis, Missouri, USA.

Non-thermal atmospheric pressure plasma-liquid synthesis of organic acids in aqueous solution from carbon monoxide

Organic acids, which were identified as intermediates in the water-gas-shift reaction, can be isolated with significant yields through plasma-liquid conversion of carbon monoxide (CO). CO results in higher oxalate and formate yields compared to carbon dioxide (CO<sub>2</sub>), bolstering the idea of a two-step conversion of CO<sub>2</sub> to organic acids *via* CO.

Image reproduced by permission of Alcina Johnson Sudagar from *Green Chem.*, 2025, **27**, 11055.

Artwork partially generated using Google Gemini and created using Canva.com.

As featured in:



See Alcina Johnson Sudagar *et al.*, *Green Chem.*, 2025, **27**, 11055.



Cite this: *Green Chem.*, 2025, **27**, 11055

## Non-thermal atmospheric pressure plasma–liquid synthesis of organic acids in aqueous solution from carbon monoxide

Alcina Johnson Sudagar, \* Piper Drebes and Elijah Thimsen

This work aims at understanding the conversion of CO to organic acids, namely oxalic acid and formic acid, using non-thermal atmospheric pressure plasma over aqueous solutions. CO exhibited significantly higher conversion to organic acids (more than 15x) compared to CO<sub>2</sub> under the same reaction conditions. The result bolsters a proposed two-step process for CO<sub>2</sub> fixation, whereby CO<sub>2</sub> is first converted to CO, and then CO is converted to organic acids. The organic acids produced from CO are intermediates in the water–gas shift (WGS) reaction of CO in the presence of an aqueous solution to dissolved CO<sub>2</sub> and hydrogen gas. Based on a simple thermodynamic analysis, the organic acid yield was increased by lowering the plasma–liquid reaction temperature using an ice bath to cool the reaction flask. The composition of the organic acids could be varied by changing the pH of the solution. Oxalate was formed in higher concentrations with increasing solution pH above the pK<sub>a</sub> of the radical species (CO<sub>2</sub>)<sup>•-</sup>. Below the pK<sub>a</sub> value, formate was the exclusive organic acid formed. The production of formate has a rather weak pH dependence but is enhanced slightly at a basic pH above 10. Furthermore, at basic pH, the effect of electrolyte concentration comes into play. Higher electrolyte concentrations, leading to shorter electrolyte Debye lengths, resulted in lowered organic acid yields. The highest yields of organic acids obtained in our system were 122 mg L<sup>-1</sup> for oxalate and 77 mg L<sup>-1</sup> for formate at an optimum 1 mM NaOH concentration in the starting solution. This work is a successful pioneering example of CO to organic acids conversion using non-thermal plasmas, which opens the pathway for a promising two-step conversion process of CO<sub>2</sub> to organic acids.

Received 23rd April 2025,  
Accepted 28th July 2025

DOI: 10.1039/d5gc02035b

[rsc.li/greenchem](https://rsc.li/greenchem)

### Green foundation

1. Our work highlights the benefit of utilizing a plasma–liquid system for converting CO to organic acids, as it alleviates reaction conditions. Plasma produces high intensities of reactive species without requiring a catalyst or chemical activators, making the industrially important organic acids production more environmentally friendly.
2. Applying low-temperature plasma improves reaction conditions by eliminating the need for high pressures and temperatures required in traditional synthesis. The plasma–liquid reaction increases desired chemical yields when CO is used as a precursor over CO<sub>2</sub>, thereby bolstering the prospect of two-step CO<sub>2</sub> conversion to organic acids *via* CO.
3. A flow-through process can be established wherein the two processes of CO<sub>2</sub> to CO conversion and CO to organic acids conversion can be built into a single setup for continuous organic acids production, thereby eliminating the collection and storage of CO gas.

## 1. Introduction

Anthropogenic greenhouse gas emissions have caused a monumental rise in global warming since the middle of the 20<sup>th</sup> century.<sup>1</sup> The major sources of CO<sub>2</sub> emissions include fuel

combustion, industrial production of cement, iron, and steel, and deforestation.<sup>2</sup> Capturing and utilizing these carbon emissions is a prospective route to decreasing the global environmental effects. Major advancements have been made in the molecular conversion of CO<sub>2</sub> into valuable organic products like esters, alkenes, acetate, acids, and alcohols.<sup>3–7</sup> The market for two organic acids, namely oxalic acid and formic acid, was 350 000 t per year and 900 000 t per year, respectively, in 2021.<sup>8</sup> They are used in industries that manufacture bleaching and cleaning agents, insecticides, metal processing, pharmaceuti-

Department of Energy, Environmental and Chemical Engineering, Washington University in Saint Louis, Saint Louis, MO 63130, USA. E-mail: [sudagar@wustl.edu](mailto:sudagar@wustl.edu), [sudagaralcinajohnson@gmail.com](mailto:sudagaralcinajohnson@gmail.com)



icals, *etc.*<sup>9</sup> There is a need to find sustainable alternative synthesis methods, such as using CO<sub>2</sub> for these acids over the currently used fossil feedstock-based methods.

The direct conversion of CO<sub>2</sub> to organic acids suffers from low reactivity as CO<sub>2</sub> is a highly stable molecule that is relatively inert under most conditions. However, there are established, relatively efficient methods to convert CO<sub>2</sub> into CO.<sup>10–14</sup> Therefore, a two-step conversion of CO<sub>2</sub> into organic acids *via* carbon monoxide (CO) is an attractive prospect. This pathway will involve first the conversion of CO<sub>2</sub> to CO and then utilizing the CO as a precursor for organic acids' syntheses. In this regard, reaction processes involving plasma technologies have been reported to improve production costs and the safety of CO gas production.<sup>13</sup> Plasma technologies also have the potential to reduce the hazard and flammability risk of CO transport by decentralizing the manufacturing of CO.<sup>13</sup> These plasma-assisted reactions have high efficiency, and the conversion process is facile.<sup>7</sup> A techno-economic analysis from 2024 has revealed the cost-effectiveness of plasma-based production of CO from CO<sub>2</sub>, wherein plasma technology advantageously lowered energy cost by nearly 43% compared to other conventional and electrochemical methods.<sup>13</sup> Furthermore, two-step electrochemistry *via* CO has been known to outperform the direct conversion of CO<sub>2</sub> to organic compounds.<sup>15</sup> Therefore, a two-step plasma-liquid reaction process has the potential to enhance production outputs and safety.

The challenge here is the conversion of CO into desired organic carbon products. Traditionally, oxalic acid has been obtained from CO using the direct dialkyl oxalate process or the indirect formate ion coupling pathway.<sup>8</sup> The dialkyl oxalate process occurs in the presence of alcohols and a Pd/ $\alpha$ -Al<sub>2</sub>O<sub>3</sub> catalyst.<sup>16</sup> In the indirect pathway, the CO is first converted into formate in the presence of caustic alkali solutions at high pressures and temperatures or using electrochemical methods.<sup>8</sup> The second step, namely, thermal conversion of formate to oxalate, also occurs at high temperatures above 400 °C and high pressures to prevent carbonate formation either with or without a catalyst. Further research has focused on using electrochemical methods as a greener pathway to achieve these organic reactions. However, the specific catalysts and electrode materials like metals (Cu, Au, Pd, Ga, Hg, Ti, and Pt),<sup>17</sup> metal oxides (MoO<sub>2</sub>, Bi<sub>2</sub>O<sub>3</sub>, Cu and Sn oxides),<sup>18,19</sup> metal-organic frameworks (metal porphyrins),<sup>20</sup> and metal-free materials (graphite and conducting polymers)<sup>20</sup> researched for efficient electrochemical applications involve the usual drawbacks of heterogenous catalysis, specifically balancing catalyst activity, catalyst stability, and cost. Plasma-liquid reactions at the electrified liquid-plasma interface involving high-energy solvated electrons and ionized species with high oxidizing or reducing power have attracted interest in sustainable chemistry.<sup>21,22</sup> Plasma-based reactors produce several orders of magnitude higher reactive species densities without any catalysts or photoactivators, making the process potentially more efficient and environmentally friendly compared to other options.<sup>23</sup> Particularly, in non-thermal atmospheric pressure plasmas, most of the electrical energy input is

directed towards energetic electrons production that subsequently produces a large variety of reactive species rather than directly heating the gas.<sup>24</sup> This emerging synthesis pathway also offers significant cost-effectiveness over electrolysis as it can eliminate the use of submerged electrodes and catalysts. Several works have been published reporting the conversion of CO<sub>2</sub> to organic acids using plasma-liquid reactions.<sup>5,25–27</sup> However, to the best of our knowledge, CO has not been applied for the plasma-liquid synthesis of organic acids like oxalate and formate.

In this work, we focused on developing a simple single-step reaction for converting CO into organic acids using a plasma-liquid approach. Our study aimed to establish that, under the same reaction conditions, CO gas results in a much higher yield of organic acids compared to CO<sub>2</sub> to validate the idea of the two-step conversion of CO<sub>2</sub> to organic acids. More than 15× higher concentrations of organic acids were obtained using CO when compared to CO<sub>2</sub> at the same reaction conditions. As the plasma activation of gases produces a variety of reactive species, we studied the prospective reaction pathways to direct the reaction in the desired route to obtain organic acids. It was found that lower reaction temperatures favored oxalate and formate formation, supporting the postulate that these organic acids are intermediates in the overall water-gas-shift (WGS) reaction of CO and water to form carbon dioxide and hydrogen. Increasing pH increases the oxalate yields, and formate production is also enhanced at a basic pH above 10. Moreover, at a high starting pH of the solution, sodium hydroxide electrolyte was more efficient in these organic reactions when compared to the other salts examined in this study. However, increasing electrolyte concentrations negatively impacted the concentration of organic acids. Therefore, optimized pH, electrolyte concentration, reaction temperature, and time were determined to obtain high organic acids yields in this system. This work paves the way towards the two-step conversion of CO<sub>2</sub> into organic acids using plasma-liquid chemistry.

## 2. Materials and methods

### 2.1. Materials

Sodium hydroxide, certified ACS grade (Fischer Scientific), sodium carbonate anhydrous, 99.5% purity (Sigma-Aldrich, USA), sulfuric acid, extra pure (Acros Organics, USA), and sodium sulfate anhydrous, certified ACS grade (Fischer Scientific, USA) were used as aqueous electrolytes. All solutions were prepared in MilliQ ultrapure water with 18.2 mΩ resistance at 25 °C produced using the Direct-Q 3 UV water purification system from Merck KGaA, USA. CO compressed gas of grade 2.5 (Linde, Canada), CO<sub>2</sub> compressed gas grade 2.5 (Praxair, USA), and Argon (Ar) compressed gas grade 5.0 (Praxair, USA) were the source gases used for producing plasma.

### 2.2. Plasma-liquid reaction setup

The non-thermal atmospheric pressure plasma-liquid reaction setup used for all experiments is shown in Fig. 1. The



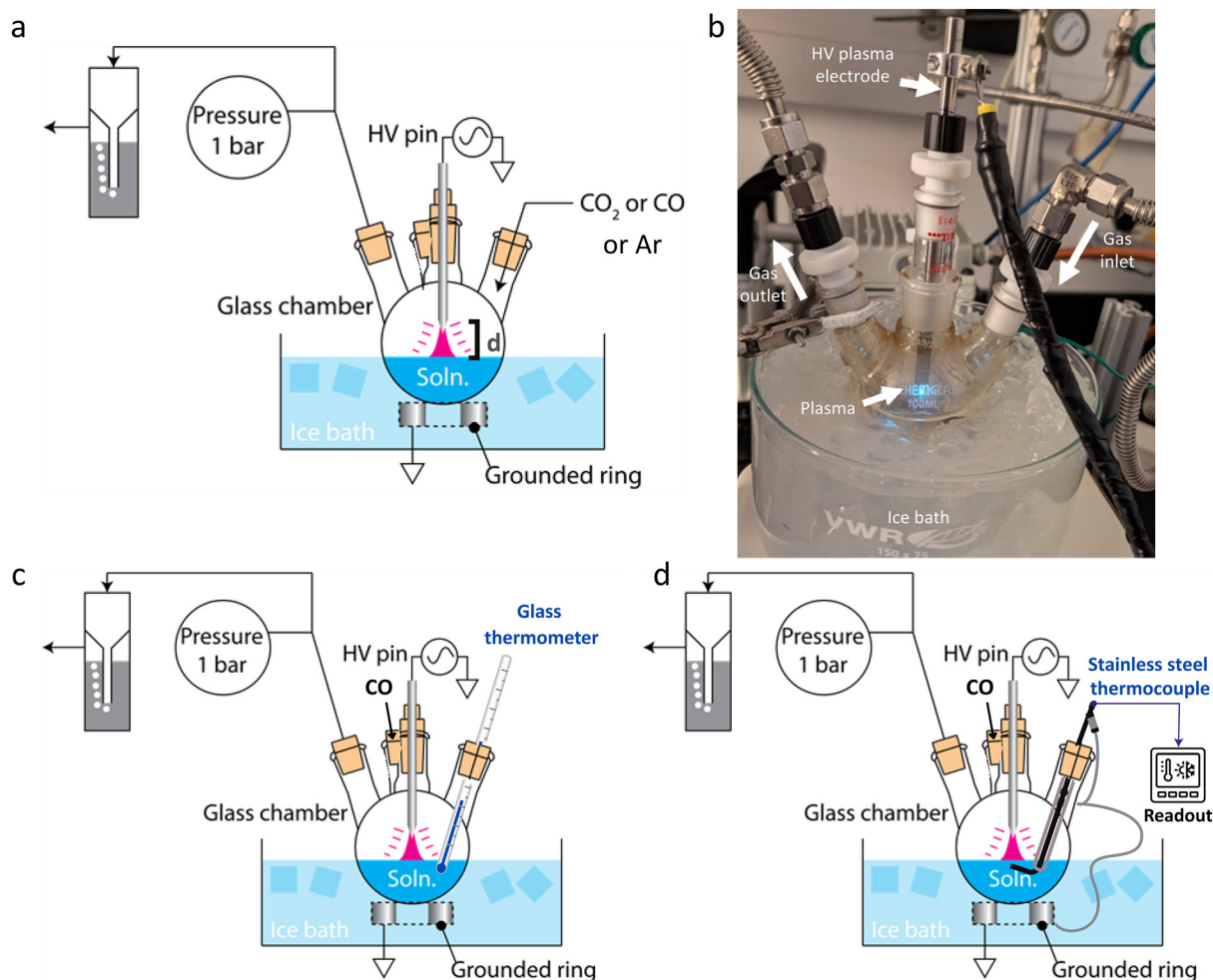


**Fig. 1** Plasma–liquid reaction experimental schematic. (a) Schematic representation of major components and (b) digital photograph of the experimental setup during non-thermal atmospheric pressure plasma–liquid reaction for organic acids synthesis. Schematic representation of modified setup for temperature measurements (c) far away ( $\sim 17$  mm distance and 10 mm depth) from the plasma–liquid reaction region and (d) close to ( $\sim 5$  mm depth) the plasma–liquid reaction region.

experiments were performed in a four-neck 100 mL round-bottom flask from ChemGlass, USA placed in a water or ice bath with one port closed. The water or ice was changed every 30 minutes to maintain the temperature conditions. A measured amount of 50 mL of electrolyte solution was used for each experiment. The system was purged using the experimental gas at 200 standard cubic centimeters per minute (scm) under 0.05 bar pressure obtained using the Insul Class F compressor from Welch, USA. The low-temperature atmospheric pressure plasma was generated using CO, CO<sub>2</sub>, or Ar as the operating gases that were passed through the round-bottom flask using a cross-flow system at a rate of 200 scm. The flow rate was controlled using a mass flow controller from MKS Instruments Inc., USA. The plasma was generated using an alternating current high-voltage (HV) power supply PVM/DDR Plasma Drive from Information Unlimited, New Hampshire, USA. The powered plasma electrode was a 316 stainless steel cylinder with a

pointed base. An aluminum ring electrode was placed on the outside of the round-bottom flask in the water or ice bath and was connected to the ground. The plasma-powered electrode was held at an optimized 2 mm distance  $d$  from the electrolyte surface (Fig. 1a). The reactions were carried out at 1 bar pressure. The plasma was generated using an input voltage of 4 kV peak-to-peak, with a frequency of 20.4 kHz, measured using a digital oscilloscope from Tektronix, USA. All experiments were conducted for 2 hours unless otherwise stated.

The non-thermal atmospheric pressure plasma is generated using one HV terminal in the gas phase and a ground electrode outside the flask. The liquid electrolyte completes the circuit. This plasma setup, which is approximately a pin-plate geometry, involves three coexisting phases: gas, liquid, and plasma. The interface between the plasma and liquid phases is called the plasma–liquid interface (PLI), where the reaction occurs. This interfacial region, generated due to the reactive



species produced in plasma injected into the liquid phase, extends only up to a few micrometers below the liquid surface,<sup>25</sup> indicating the localized reaction volume of the plasma–liquid reactions.

The temperature variation during the reaction was measured at two distinct regions inside the flask as shown in Fig. 1c and d. For these experiments, the fourth port was utilized. An Accu-Safe N16B glass thermometer from Thermco Product Inc., USA was used for temperature monitoring far away, approximately 17 mm distance and 10 mm depth from the plasma–liquid interface region (Fig. 1c). A modified stainless steel probe K-type thermocouple from Omega, USA, was used to determine the temperature of the solution close to the plasma–liquid interface region (~5 mm below the surface) as seen in Fig. 1d. The modified probe was prepared by adding a glass sheath for insulating the part of the probe outside the liquid and bending the bottom 15 mm of the probe at a 90° angle to reach the plasma–liquid interface region. Temperatures were recorded during two hours of reaction time for reactions occurring in an ice bath kept at  $4 \pm 1$  °C and a water bath kept at  $25 \pm 3$  °C. Both regions inside the flask exhibited similar steady-state temperatures during the two-hour reaction time. In the case of an ice bath used to cool the reaction flask, the solution temperature rose over 10 minutes to the steady state value of  $22 \pm 2$  °C that was the same both close to the plasma and far away. In the case of an ambient temperature water bath used to cool the reaction flask, the solution temperature rose over 20 minutes to the steady state value of  $41 \pm 2$  °C that was also the same both close to the plasma and far away.

### 2.3. Products analyses

**Dissolved ions analysis.** Dissolved anions [ $\text{HCO}_2^-$  and  $(\text{CO}_2)_2^{2-}$ ] in the products obtained after the plasma reaction were analyzed using a conductivity detector in the Thermo Scientific Dionex Integriion High-Pressure Ion Chromatograph (IonC), applying a gradient increase in the eluent KOH concentration from 0.5 to 38.8 mM between 0 and 20 minutes. The anion concentrations in the unacidified aqueous solutions were determined using the analytical AS19 Dionex IonPac™ column at the temperature of 30 °C with the eluent generated from an eluent generator Dionex cartridge (EGC 500 KOH). The flow rate was kept constant at 1 mL  $\text{min}^{-1}$ . Sodium formate, purity  $\geq 99\%$  (Sigma Aldrich, USA), and sodium oxalate, purity  $\geq 99.5\%$  (Sigma Aldrich, USA), standards were used for obtaining calibration curves. The curves were used for the calculation of the concentration of these compounds in the plasma reaction samples. The calibration curves were obtained when the area under the curve for the peaks obtained at designated retention times (~3.2 min for formate ion and ~10.7 min for oxalate ion) was plotted against the known millimolar concentrations of the standards. The concentrations of the products in the reaction samples were converted from  $\text{mM L}^{-1}$  to  $\text{mg L}^{-1}$  using the molecular mass of formate ( $45.015 \text{ g mol}^{-1}$ ) and oxalate ( $88.018 \text{ g mol}^{-1}$ ) ions. A linear fit with  $R^2 \geq 0.999$  was

obtained for both formate and oxalate curves in the concentration range of 1–140  $\text{mg L}^{-1}$  for formate and 2–245  $\text{mg L}^{-1}$  for oxalate (Fig. S1). Reactions were repeated in triplicate to check reproducibility, and a standard deviation of less than 4  $\text{mg L}^{-1}$  was obtained.

**Total inorganic carbon analysis.** The total inorganic carbon was detected and quantified using the liquid total organic carbon (TOC) analyzer (TOC-L, Shimadzu, Japan). For the inorganic carbon (IC) analysis, the samples were acidified using a 20% phosphoric acid solution, and the  $\text{CO}_2$  bubbles produced by IC were carried to the non-dispersive infrared detector for analysis. The carbon content obtained using the TOC analyzer was averaged over three measurements. The method developed for obtaining the standard calibration plots consisted of preparing a stock solution with sodium carbonate and sodium formate in 10 mM NaOH. The calibration curves were obtained using the auto-dilution feature of the analyzer and plotting the area under the curve against known concentrations of the standards. The solutions were acidified in the analyzer using a 1.5% 1 M hydrochloric acid prior to analysis. The concentrations of the inorganic products in the reaction samples were converted from  $\text{mg L}^{-1}$  of carbon to  $\text{mg L}^{-1}$  by using the molecular mass of the carbonate ( $60.008 \text{ g mol}^{-1}$ ) ion.

**pH analysis.** The pH analysis was performed using the Orhaus Aquasearcher with the ST310 pH electrode. The measurements were performed in triplicate after a 1 minute equilibration time, and pH values were averaged. The standard Orhaus buffer solutions with pH 4, 7, and 10 at 25 °C were used for calibration. The pH 4.01 buffer solution contained potassium hydrogen phthalate, the pH 7.01 buffer solution contained disodium hydrogen phosphate and potassium dihydrogen phosphate, and the pH 10.01 buffer solution contained sodium carbonate and sodium bicarbonate. The pH of all solutions was measured after the solutions reached room temperature.

## 3. Results and discussion

The plasma–liquid reaction produced significantly more organic acid when CO was used as the source gas instead of  $\text{CO}_2$ . Comparative reactions were performed using CO and  $\text{CO}_2$  as source gas for otherwise identical reaction conditions. The reactions were performed at a lower temperature of  $22 \pm 2$  °C for 2 hours near the plasma liquid interface of the aqueous solution initially containing 1 mM NaOH electrolyte with a starting pH of 11. Ion chromatography analysis was used for determining the oxalate and formate yields and carbonates were quantified using the total organic carbon analyzer (ion chromatograms in Fig. S2a). Formate, oxalate, and carbonate were detected in both CO and  $\text{CO}_2$ -based plasma–liquid reactions (Table S1). In comparison with  $\text{CO}_2$  as source gas (1.6  $\text{mg L}^{-1}$  formate and 4.4  $\text{mg L}^{-1}$  oxalate), the CO plasma–liquid reaction yielded about 15× higher amounts of oxalate (69.5  $\text{mg L}^{-1}$ ) and about 30× higher amounts of formate



(49.5 mg L<sup>-1</sup>, Fig. 2), indicating significantly higher organic acids yields when CO gas was used as the source. This result suggests that a two-step process whereby CO<sub>2</sub> is first converted to CO, and then CO is converted to organic acids, will yield higher organic acids (oxalate and formate) than the direct use of CO<sub>2</sub> in a plasma-liquid reaction, provided the production of CO from CO<sub>2</sub> is reasonably efficient.

Secondly, the organic acids appear to be intermediates in the WGS reaction when CO is used as the source gas for the plasma-liquid reaction. About 13.6 mg L<sup>-1</sup> carbonates were detected in the ending solution, wherein CO was used as the source gas (Table S1). However, the pH of the solution (3.6) obtained after the CO source gas-based reaction was significantly lower than the pK<sub>a</sub> of carbonic acid (6.3), so carbonates may escape the solution as CO<sub>2</sub>. Analysis of the product gas collected downstream in an NaOH scrubber after the reaction showed that about 618 mg L<sup>-1</sup> of carbonates were produced during the reaction for up to 2 hours. This large amount of inorganic carbonates formed during the reaction supports the postulate that the conversion of CO at the non-thermal atmospheric pressure PLI in the presence of an aqueous solution follows the water-gas shift reaction:



The organic acids (oxalate and formate) we detect are the intermediates of this WGS reaction. The goal is, therefore, to maximize the formation of these intermediates since they are the desired compounds.

As the WGS reaction proceeds *via* the oxalate and formate intermediates (eqn (1)), the reaction has two steps, namely, the conversion of CO to organic acid intermediates and the decomposition of the intermediates to carbonate in the aqueous solution. Standard Gibbs free energy and enthalpy

of reactions calculated for the formation and decomposition of organic intermediates oxalate and formate in the WGS reaction can be seen in Table 1. The thermodynamic expectation is a higher organic acid yield if the reaction temperature is lowered since the formation of oxalate and formate from CO is exothermic and endergonic at ambient temperature, while their decomposition into CO<sub>2</sub> is endothermic and exergonic at ambient temperature. The plasma-liquid reaction produced significantly more organic acid when the temperature of the aqueous solution was maintained at an overall low temperature of 22 ± 2 °C (Fig. 3 and ion chromatograms in Fig. S2b). Experiments were conducted in which everything was kept the same, but in one case, the reaction vessel was immersed in an ice bath (4 ± 1 °C) that maintained the aqueous solution temperature at 22 ± 2 °C, while in the other case, it was immersed in an ambient temperature water bath (25 ± 3 °C) that maintained the solution temperature at 41 ± 2 °C. The reactions were performed with continuous CO gas flow for 2 hours near the PLI of the 10 mM NaOH aqueous electrolyte solution with a starting pH of 12. The result of the experiment was 2.5× higher formate (29 mg L<sup>-1</sup>) and more than 4× higher oxalate (12 mg L<sup>-1</sup>) in the lower temperature

**Table 1** Standard Gibbs free energies and enthalpies of reactions calculated for the formation and decomposition of organic compounds formate and oxalate

Index	Reaction	$\Delta H_{\text{rxn}}^{\circ}$ (298 K)	$\Delta G_{\text{rxn}}^{\circ}$ (298 K)
1	$\text{CO}_{(g)} + \text{H}_2\text{O}_{(l)} \rightarrow \text{H}_2\text{CO}_{2(l)} + \text{H}_2(g)$	-28.7	+13.0
2	$2\text{CO}_{(g)} + 2\text{H}_2\text{O}_{(l)} \rightarrow \text{H}_2(\text{CO}_2)_{2(s)} + \text{H}_2(g)$	-36.3	+50.0
3	$\text{H}_2(\text{CO}_2)_{2(s)} \rightarrow 2\text{CO}_{2(g)} + \text{H}_2(g)$	+40.2	-90.8
4	$\text{H}_2(\text{CO}_2)_{2(l)} \rightarrow \text{CO}_{2(g)} + \text{H}_2(g)$	+31.5	-33.0



**Fig. 2** CO process gas produced more organic acids than CO<sub>2</sub>. Mass concentration of oxalate (blue) and formate (magenta) as measured by ion chromatography for CO<sub>2</sub> and CO process gas. The initial electrolyte composition was 1 mM NaOH.

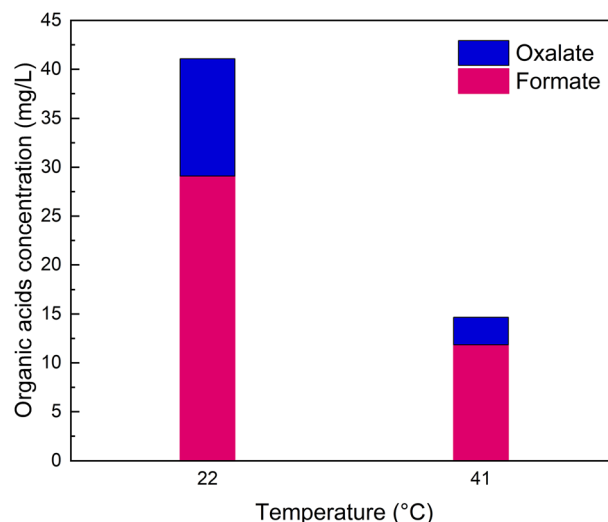


**Fig. 3** A higher yield of organic acids was obtained at lower solution temperature. Mass concentration of oxalate (blue) and formate (magenta) as measured by ion chromatography for reactions at lower (22 ± 2 °C) and higher (41 ± 2 °C) temperatures. The initial electrolyte composition was 10 mM NaOH.



( $22 \pm 2$  °C) reaction compared to the reaction at  $41 \pm 2$  °C ( $11.9$  mg L<sup>-1</sup> formate and  $2.8$  mg L<sup>-1</sup> oxalate) even though the plasma generation conditions, and reaction conditions (reaction time and initial electrolyte) were the same. Moreover, the lowered yield of organic acids at  $41 \pm 2$  °C was complemented by an increase in carbonates (Table S1), suggesting that the organic acid decomposition was more extensive at the higher temperature, consistent with the thermodynamic expectation. Therefore, a lower reaction temperature of  $22 \pm 2$  °C was used for the remainder of the study. The result is consistent with the overall reaction being a WGS reaction that proceeds through oxalate and formate intermediates.

The starting pH of the solution significantly affects oxalate yields, whereas its effect on formate production is rather weak in a plasma-liquid reaction. A monotonic increase in oxalate yield was observed when the pH of the starting solution was increased from 1.9 to 11 (Fig. 4a and ion chromatograms in Fig. S3). For formate, this increase in yield was rather subtle. Experiments were performed using electrolyte concentration with different starting pH values between 2 and 12. The electrolytes used were 10 mM NaOH (pH 12), 1 mM NaOH (pH 11), 0.5 mM NaOH (pH 10.7), 1 mM Na<sub>2</sub>CO<sub>3</sub> (pH 10), 1 mM Na<sub>2</sub>SO<sub>4</sub> (pH 5.7), and 1 mM H<sub>2</sub>SO<sub>4</sub> (pH 2.7). An even lower pH was obtained using a 5 mM H<sub>2</sub>SO<sub>4</sub> (pH 1.9). The pH attained in each case after the reaction can be seen in Table S1. All other experimental parameters, including the plasma and reaction conditions, were kept the same for all experiments. Oxalate production decreased with decreasing pH and completely disappeared below pH 2, even though all other plasma and reaction conditions were kept the same. Therefore, to obtain oxalate, a pH higher than 2 is essential. This obser-

vation is consistent with previously published reports of oxalate formation wherein the reaction pathway is *via* the pH-dependent CO<sub>2</sub><sup>•-</sup> radical species.<sup>28</sup> The highest oxalate ( $69.5$  mg L<sup>-1</sup>) yield was obtained when 1 mM NaOH was used as the electrolyte with a starting pH of 11.

The formate yield, disparately, did not dramatically vary between pH 1.9 and 6 but was enhanced by basic pH of 10 and above (Fig. 4a). The highest formate yield of  $77$  mg L<sup>-1</sup> was also obtained for an initially 1 mM NaOH electrolyte with pH 11. Unlike oxalate, the formate production did not get cut off at either acidic or basic pH but only varied in concentration, indicating the formation of formate is *via* a reactive species that is weakly affected by pH. Conclusively, high pH favors the formation of both organic acids. This observation is in accordance with previously reported literature on the thermochemical synthesis of organic acids, wherein the WGS reaction was enhanced in the presence of hydroxyl and carbonate anions.<sup>29</sup>

However, a further increase in pH up to 12.7 was unfavorable for oxalate and formate production due to the high electrolyte concentrations necessary to obtain these higher starting solution pH values (Fig. 4b and ion chromatograms in Fig. S4). Reactions were performed using different concentrations (1, 10, and 20 mM) of two electrolytes, namely, Na<sub>2</sub>CO<sub>3</sub> and NaOH, while keeping all other reaction and plasma generation conditions the same. A significant drop in the organic acids production was observed when the electrolyte concentration was increased from 1 to 10 mM in the case of both the electrolytes Na<sub>2</sub>CO<sub>3</sub> and NaOH. The organic acid yields further decreased when the electrolyte concentrations were increased to 20 mM. This observation can be related to the electrolyte Debye length. In previous work, we elucidated the dependence of the reduction potential on electrolyte Debye length in

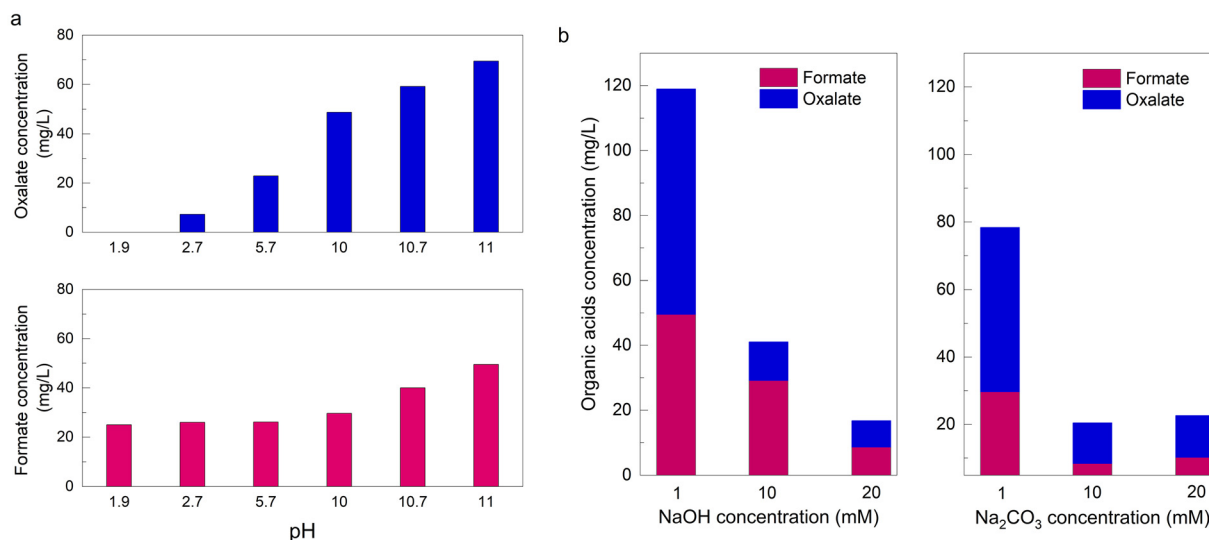


**Fig. 4** (a) A monotonic increase in oxalate and formate yields with increasing starting pH of the solution. (b) A monotonic decrease in oxalate and formate yields with increasing electrolyte concentration of the solution. Mass concentration of oxalate (blue) and formate (magenta) as measured by ion chromatography for reactions at different starting pH of the solution. The electrolytes used were 5 mM H<sub>2</sub>SO<sub>4</sub> (pH 1.9), 1 mM H<sub>2</sub>SO<sub>4</sub> (pH 2.7), 1 mM Na<sub>2</sub>SO<sub>4</sub> (pH 5.7), 1 mM Na<sub>2</sub>CO<sub>3</sub> (pH 10), 0.5 mM NaOH (pH 10.7), 1 mM NaOH (pH 11), 10 mM Na<sub>2</sub>CO<sub>3</sub> (pH 11.4), 20 mM Na<sub>2</sub>CO<sub>3</sub> (pH 11.7), 10 mM NaOH (pH 12) and 20 mM NaOH (pH 12.7).



plasma–liquid systems.<sup>30</sup> The electrolyte Debye length is representative of the scale over which charge screening occurs in solution. Based on the work by Oldham *et al.*, at low electrolyte concentrations of 1 mM, longer electrolyte Debye lengths lead to more negative reduction potentials in solution.<sup>30</sup> The more negative reduction potential at lower electrolyte concentration is expected to enhance organic acid synthesis reactions. In other words, when the electrolyte concentration increases, the Debye length gets shorter, and the driving force for reduction reactions is weaker. The less negative reduction potential expected at high electrolyte concentrations is consistent with the decrease in organic acid yields at electrolyte concentrations greater than 1 mM.

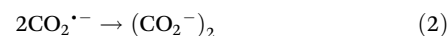
With increasing reaction time, the oxalate and formate concentrations reached a steady state value in a 1 mM NaOH aqueous solution, consistent with the idea that these species are intermediates in the WGS reaction. Plasma–liquid reactions were performed in the optimized 1 mM NaOH solution for up to 18 hours while keeping all other reaction conditions identical. A steep increase in organic acids production can be seen up to 4 hours reaction time. The steady state was reached after approximately 10 hours (Fig. 5 and ion chromatograms in Fig. S5). The pH value at the steady state was greater than 3.0. The steady-state oxalate concentration was  $\sim 122$  mg L<sup>-1</sup>, and the formate concentration was 77 mg L<sup>-1</sup>.

Control experiments were conducted with Ar plasma gas instead of CO, and formate, oxalate or carbonate initially added to test hypotheses about the behavior of these species in solution (Fig. S6). In one case, sodium formate was initially added to the 1 mM NaOH solution to observe if it reacted to form any other organic compounds. Similarly, in another experiment, sodium oxalate was added, and in a third experiment, sodium carbonate was added initially to 1 mM NaOH

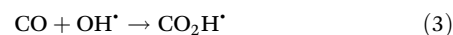
solution before starting the reaction. When oxalate and formate were initially present, these compounds were found to decompose into carbonates, but no other species were detected in the product mixture, eliminating a hypothetical conversion of oxalate and formate into other organic acids. The product mixture from the experiment with initially added carbonates also did not contain any other compounds, eliminating a hypothetical conversion of inorganic carbon to organic acids without CO. This result indicates that CO-derived intermediate species are crucial for driving the production of organic acids in a non-thermal atmospheric pressure plasma–liquid reaction.

The experimental observations in the conversion of CO to organic acids at the PLI yield an understanding of the possible mechanistic pathways involved in the formation of formate and oxalate in aqueous solutions. The conversion of CO to organic acids involves a gas-phase reaction that converts the CO gas to an excited state through plasma activation. The excited state of CO denoted by CO\* produces species like C, O, CO<sub>2</sub>, and C<sub>2</sub>O and can also give rise to CO<sub>2</sub>H\* and HCO\* radical species in the presence of water based on research reported in the field of radiolysis.<sup>31,32</sup> The gas phase reactions can also involve the WGS, leading to the production of CO<sub>2</sub> and H<sub>2</sub>. Plasma activation also produces other highly active species, including hydrated e<sup>-</sup>, OH\*, H<sub>2</sub>O<sub>2</sub>, H\*, and O<sub>2</sub>\*<sup>-</sup>.<sup>33</sup> Reactions following plasma activation lead to reactive species like CO<sub>2</sub>H\* and HCO\*, which are crucial to determining the end products.

In traditional synthesis methods, oxalate is obtained from CO through the formate coupling reaction wherein two formate ions react to form oxalate *via* the carbonite (CO<sub>2</sub><sup>2-</sup>) pathway.<sup>34</sup> In this method, the oxalate formation is observed only for alkali formates.<sup>8</sup> However, in the case of non-thermal plasma–liquid synthesis, the oxalate is formed at pH values much lower than the pK<sub>a</sub> of the formate ion, indicating that oxalate production follows a different pathway. The reaction pathway observed for the oxalate synthesis is anticipated to be formed by the rapid recombination of the deprotonated form of the CO<sub>2</sub>H\* radical.<sup>32</sup>



This radical species can be formed by the reaction of CO with hydroxyl radical.<sup>28</sup>



The radical species is an acid and thus has two forms depending on the pH conditions.<sup>26,28,32</sup>



The pK<sub>a</sub> of the radical species (CO<sub>2</sub>)<sup>\*·</sup> has been studied with values reported over the range from 1.4 to 3.9.<sup>28</sup> Pulse radiolysis with conductometric detection yielded a pK<sub>a</sub> value of 3.9.<sup>32</sup> This measurement was repeated by another group and a different value was presented to be 2.3.<sup>28</sup> The Raman spectra-based analysis yielded a pK<sub>a</sub> value of 3.4.<sup>35</sup> Previous literature

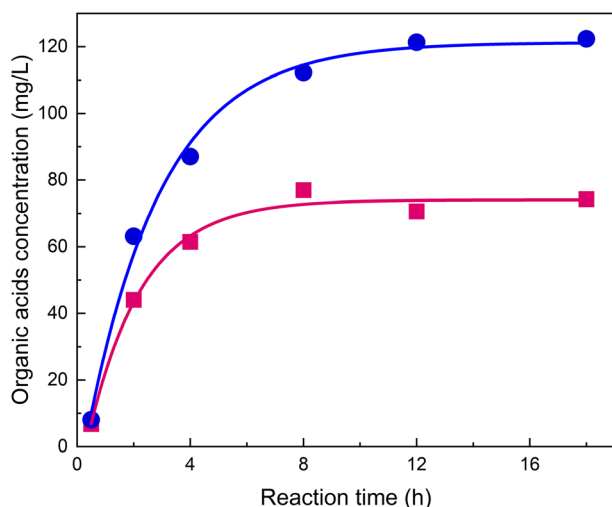
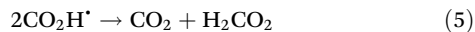


**Fig. 5** Steady state of organic acid concentration indicates these species are intermediates in the overall water gas shift reaction. The initial electrolyte concentration was 1 mM NaOH. Mass concentration of oxalate as measured by ion chromatography for different reaction times at 1 mM NaOH.



has also reported values of  $-0.2$  and  $1.4$ , which were considered to contain some artifacts in measurement methods.<sup>28,36,37</sup> However, according to our reaction outcomes, a very low oxalate yield was obtained at pH 2.7, and no oxalate was formed at pH 1.9. Therefore, our results suggest that the  $pK_a$  lies between values of 1.9 and 2.7, which is closely related to the reported value of 2.3 by Flyunt *et al.*, obtained using pulse radiolysis and conductometric detection.<sup>28</sup> Below the  $pK_a$  value, the intermediate has the form  $CO_2H^*$ , which undergoes disproportionation to yield formic acid.<sup>28</sup>



This shows that oxalate formation can be effectively controlled simply by changing the pH of the aqueous solution in a plasma-liquid reaction.

Furthermore, in CO-based plasma reaction, we see significant formate production at all pH unlike that observed for  $CO_2$  reported previously by Rumbach *et al.*<sup>26</sup> In their case, the formate is only formed in significant amounts at acidic pH below the  $pK_a$  of  $CO_2^{*-}$ . However, in our case, the formate is obtained from CO through an undetermined weakly pH-dependent reactive species.

Oxalate and formate have been observed to act as intermediates in the thermochemical conversion of CO to  $CO_2$  and  $H_2$ , which has been enhanced in the presence of an alkaline solution containing hydroxide or carbonates at temperatures above 200 °C.<sup>38–40</sup> In our case as well, basic pH favors organic acids formation. Importantly, high pressures and temperatures have been essential for driving the WGS *via* the formate and oxalate intermediates in traditional synthesis methods. Non-thermal atmospheric pressure plasma activation of the reactant CO eliminates the need for a heterogeneous catalyst and harsh reaction conditions like high temperature and pressure for obtaining the organic acids, which is expected to be beneficial when working with an aqueous solution. Particularly, oxalic acid is directly obtained in a one-step process from CO, which traditionally requires a two-step synthesis process in thermochemical methods.

## 4. Conclusion

This work is proof of concept that CO is a promising starting source for organic acid syntheses when compared to  $CO_2$ . The CO plasma-liquid reaction produces about 15× higher amounts of oxalate and 30× higher amounts of formate compared to a  $CO_2$  plasma under otherwise identical conditions. This exhibits potential for a two-step conversion of  $CO_2$  to organic acids *via* CO wherein the  $CO_2$  can be first converted to CO through plasma/thermochemical/electrochemical methods widely reported in literature, and the CO produced can be used as a precursor for the organic acids synthesis as described in this work. Further, the organic acids oxalate and formate are intermediates in the water-gas-shift reaction, and hence their yields can be increased by lowering the reaction temperature to promote production over decomposition.

Oxalate appears to be formed *via* the pH-dependent  $CO_2^{*-}$  radical species, and therefore, the concentration of oxalate formed can be effectively controlled by varying the pH of the solution. Contrarily, the formation of formate is weakly dependent on pH and was obtained under all pH values explored in this work but was enhanced under basic pH conditions. At basic pH, the water-gas-shift reaction becomes pronounced, leading to higher oxalate and formate production. However, above an optimum electrolyte concentration (1 mM), the shorter electrolyte Debye lengths led to decreased yields of oxalate and formate. Therefore, by running the reaction at lower temperatures and a basic pH of 11, the highest oxalate ( $122 \text{ mg L}^{-1}$ ) and formate ( $77 \text{ mg L}^{-1}$ ) yields can be obtained in our system. Although further advancement in the system is required for producing industry-relevant amounts of organic acids, the plasma-liquid reactions operate under mild conditions and do not require heterogeneous catalysts, making them attractive options for research as potential industrial processes.

## Conflicts of interest

There are no conflicts to declare.

## Data availability

The data supporting the findings of this study are available in the article's main text and SI.

Supplementary information is available. The SI includes calibration plots (Fig. S1) for Ion Chromatography analysis of organic acids, ion chromatograms (Fig. S2–S6), and a comprehensive analysis table (Table S1) supporting the results discussed in the main text. See DOI: <https://doi.org/10.1039/d5gc02035b>

## Acknowledgements

This project was funded in part by the United States National Science Foundation through award CBET 2033714 and the United States Department of Energy through award DE-SC0020352. We thank Dr Elaine Flynn from the Department of Earth, Environmental, and Planetary Sciences at Washington University in St. Louis for the method development and troubleshooting of Ion Chromatography experiments.

## References

- 1 R. Lindsey, Climate Change: Atmospheric Carbon Dioxide, 2024. <https://www.climate.gov/news-features/understanding-climate/climate-change-atmospheric-carbon-dioxide>, (accessed 2024-07-30).
- 2 Greenhouse Gas Emissions, 2024, <https://www.epa.gov/ghgemissions/overview-greenhouse-gases>, (accessed 2024-07-30).



- 3 C. A. R. Pappijn, M. Ruitenbeek, M. F. Reyniers and K. M. Van Geem, Challenges and Opportunities of Carbon Capture and Utilization: Electrochemical Conversion of CO<sub>2</sub> to Ethylene, *Front. Earth Sci.*, 2020, **8**, 557466, DOI: [10.3389/fenrg.2020.557466](https://doi.org/10.3389/fenrg.2020.557466).
- 4 A. Jana, S. W. Snyder, E. J. Crumlin and J. Qian, Integrated Carbon Capture and Conversion: A Review on C<sub>2</sub>+ Product Mechanisms and Mechanism-Guided Strategies, *Front. Chem.*, 2023, **11**, 1135829, DOI: [10.3389/fchem.2023.1135829](https://doi.org/10.3389/fchem.2023.1135829).
- 5 S. Paulussen, B. Verheyde, X. Tu, C. De Bie, T. Martens, D. Petrovic, A. Bogaerts and B. Sels, Conversion of Carbon Dioxide to Value-Added Chemicals in Atmospheric Pressure Dielectric Barrier Discharges, *Plasma Sources Sci. Technol.*, 2010, **19**(3), 034015, DOI: [10.1088/0963-0252/19/3/034015](https://doi.org/10.1088/0963-0252/19/3/034015).
- 6 H. Radhakrishnan, S. Gnanbe, A. Duereh, S. U. Iffat Uday, A. Lusi, H. Hu, H. Hu, M. M. Wright and X. Bai, Non-Equilibrium Plasma Co-Upcycling of Waste Plastics and CO<sub>2</sub> for Carbon-Negative Oleochemicals, *Green Chem.*, 2024, **26**(16), 9156–9175, DOI: [10.1039/d4gc02340d](https://doi.org/10.1039/d4gc02340d).
- 7 H. Puliyalil, D. Lašič Jurković, V. D. B. C. Dasireddy and B. Likozar, A Review of Plasma-Assisted Catalytic Conversion of Gaseous Carbon Dioxide and Methane into Value-Added Platform Chemicals and Fuels, *RSC Adv.*, 2018, **8**(48), 27481–27508, DOI: [10.1039/c8ra03146k](https://doi.org/10.1039/c8ra03146k).
- 8 E. Schuler, M. Demetriou, N. R. Shiju and G. J. M. Gruter, Towards Sustainable Oxalic Acid from CO<sub>2</sub> and Biomass, *ChemSusChem*, 2021, **14**(18), 3636–3664, DOI: [10.1002/cssc.202101272](https://doi.org/10.1002/cssc.202101272).
- 9 Y. Xu, S. Li and H. Fang, Direct Synthesis of Oxalic Acid via Oxidative CO Coupling Mediated by a Dinuclear Hydroxycarbonylcobalt(III) Complex, *Nat. Commun.*, 2023, **14**(1), 2739, DOI: [10.1038/s41467-023-38442-4](https://doi.org/10.1038/s41467-023-38442-4).
- 10 Y. Yin, T. Yang, Z. Li, E. Devid, D. Auerbach and A. W. Kleyn, CO<sub>2</sub> Conversion by Plasma: How to Get Efficient CO<sub>2</sub> Conversion and High Energy Efficiency, *Phys. Chem. Chem. Phys.*, 2021, **23**(13), 7974–7987, DOI: [10.1039/d0cp05275b](https://doi.org/10.1039/d0cp05275b).
- 11 R. Snoeckx and A. Bogaerts, Plasma Technology—a Novel Solution for CO<sub>2</sub> Conversion?, *Chem. Soc. Rev.*, 2017, **46**(19), 5805–5863, DOI: [10.1039/c6cs00066e](https://doi.org/10.1039/c6cs00066e).
- 12 H. Kildahl, L. Wang, L. Tong, H. Cao and Y. Ding, Industrial Carbon Monoxide Production by Thermochemical CO<sub>2</sub> Splitting - A Techno-Economic Assessment, *J. CO<sub>2</sub> Util.*, 2022, **65**, 102181, DOI: [10.1016/j.jcou.2022.102181](https://doi.org/10.1016/j.jcou.2022.102181).
- 13 J. Osorio-Tejada, M. Escriba-Gelonch, R. Vertongen, A. Bogaerts and V. Hessel, CO<sub>2</sub> Conversion to CO via Plasma and Electrolysis: A Techno-Economic and Energy Cost Analysis, *Energy Environ. Sci.*, 2024, 5833–5853, DOI: [10.1039/d4ee00164h](https://doi.org/10.1039/d4ee00164h).
- 14 J. L. Liu, X. Wang, X. S. Li, B. Likozar and A. M. Zhu, CO<sub>2</sub> Conversion, Utilisation and Valorisation in Gliding Arc Plasma Reactors, *J. Phys. D: Appl. Phys.*, 2020, **53**(25), 253001, DOI: [10.1088/1361-6463/ab7c04](https://doi.org/10.1088/1361-6463/ab7c04).
- 15 J. Li, F. Che, Y. Pang, C. Zou, J. Y. Howe, T. Burdyny, J. P. Edwards, Y. Wang, F. Li, Z. Wang, P. De Luna, C. T. Dinh, T. T. Zhuang, M. I. Saidaminov, S. Cheng, T. Wu, Y. Z. Finfrock, L. Ma, S. H. Hsieh, Y. S. Liu, G. A. Botton, W. F. Pong, X. Du, J. Guo, T. K. Sham, E. H. Sargent and D. Sinton, Copper Adparticle Enabled Selective Electrosynthesis of N-Propanol, *Nat. Commun.*, 2018, **9**(1), 4614, DOI: [10.1038/s41467-018-07032-0](https://doi.org/10.1038/s41467-018-07032-0).
- 16 C. Wang, X. Li, S. Yuan, L. Sun, P. Bai, L. Ling, H. Guo and S. Mintova, Oxidative Coupling of Carbon Monoxide to Dimethyl Oxalate: Catalysts Design, Reaction Mechanism and Process Intensification, *Catal. Rev. Sci. Eng.*, 2024, **67**, 323–370, DOI: [10.1080/01614940.2024.2320165](https://doi.org/10.1080/01614940.2024.2320165).
- 17 J. Durst, A. Rudnev, A. Dutta, Y. Fu, J. Herranz, V. Kaliginedi, A. Kuzume, A. A. Permyakova, Y. Paratcha, P. Broekmann and T. J. Schmidt, Electrochemical CO<sub>2</sub> Reduction - A Critical View on Fundamentals, Materials and Applications, *Chimia*, 2015, **69**(12), 769–776, DOI: [10.2533/chimia.2015.769](https://doi.org/10.2533/chimia.2015.769).
- 18 Y. Oh, H. Vrabel, S. Guidoux and X. Hu, Electrochemical Reduction of CO<sub>2</sub> in Organic Solvents Catalyzed by MoO<sub>2</sub>, *Chem. Commun.*, 2014, **50**(29), 3878–3881, DOI: [10.1039/c3cc49262a](https://doi.org/10.1039/c3cc49262a).
- 19 J. Li, S. U. Abbas, H. Wang, Z. Zhang and W. Hu, Recent Advances in Interface Engineering for Electrocatalytic CO<sub>2</sub> Reduction Reaction, *Nano-Micro Lett.*, 2021, **13**(1), 216, DOI: [10.1007/s40820-021-00738-9](https://doi.org/10.1007/s40820-021-00738-9).
- 20 J. Lin, Y. Zhang, P. Xu and L. Chen, CO<sub>2</sub> Electrolysis: Advances and Challenges in Electrocatalyst Engineering and Reactor Design, *Mater. Rep.: Energy*, 2023, **3**(2), 100194, DOI: [10.1016/j.matre.2023.100194](https://doi.org/10.1016/j.matre.2023.100194).
- 21 P. Rumbach, D. M. Bartels, R. M. Sankaran and D. B. Go, The Solvation of Electrons by an Atmospheric-Pressure Plasma, *Nat. Commun.*, 2015, **6**, 7248, DOI: [10.1038/ncomms8248](https://doi.org/10.1038/ncomms8248).
- 22 H. Hosseini, An Overview of Chemical Reactions Activated by Plasma, *Ind. Eng. Chem. Res.*, 2024, **63**, 19418–19434, DOI: [10.1021/acs.iecr.4c02506](https://doi.org/10.1021/acs.iecr.4c02506).
- 23 J. Wang, N. B. Üner, S. E. Dubowsky, M. P. Confer, R. Bhargava, Y. Sun, Y. Zhou, R. M. Sankaran and J. S. Moore, Plasma Electrochemistry for Carbon-Carbon Bond Formation via Pinacol Coupling, *J. Am. Chem. Soc.*, 2023, **145**(19), 10470–10474, DOI: [10.1021/jacs.3c01779](https://doi.org/10.1021/jacs.3c01779).
- 24 A. Fridman, A. Chirokov and A. Gutsol, Non-Thermal Atmospheric Pressure Discharges, *J. Phys. D: Appl. Phys.*, 2005, **38**(2), DOI: [10.1088/0022-3727/38/2/R01](https://doi.org/10.1088/0022-3727/38/2/R01).
- 25 A. Mota-Lima, The Electrified Plasma/Liquid Interface as a Platform for Highly Efficient CO<sub>2</sub> Electroreduction to Oxalate, *J. Phys. Chem. C*, 2020, **124**(20), 10907–10915, DOI: [10.1021/acs.jpcc.0c00099](https://doi.org/10.1021/acs.jpcc.0c00099).
- 26 P. Rumbach, R. Xu and D. B. Go, Electrochemical Production of Oxalate and Formate from CO<sub>2</sub> by Solvated Electrons Produced Using an Atmospheric-Pressure Plasma, *J. Electrochem. Soc.*, 2016, **163**(10), F1157–F1161, DOI: [10.1149/2.0521610jes](https://doi.org/10.1149/2.0521610jes).



- 27 B. Eliasson, C. J. Liu and U. Kogelschatz, Direct Conversion of Methane and Carbon Dioxide to Higher Hydrocarbons Using Catalytic Dielectric-Barrier Discharges with Zeolites, *Ind. Eng. Chem. Res.*, 2000, **39**(5), 1221–1227, DOI: [10.1021/ie990804r](https://doi.org/10.1021/ie990804r).
- 28 R. Flyunt, M. N. Schuchmann and C. Von Sonntag, A Common Carbanion Intermediate in the Recombination and Proton-Catalysed Disproportionation of the Carboxyl Radical Anion, CO<sub>2</sub>·<sup>-</sup>, in Aqueous Solution, *Chem. – Eur. J.*, 2001, **7**(4), 796–799, DOI: [10.1002/1521-3765\(20010216\)7:4<796::AID-CHEM796>3.0.CO;2-J](https://doi.org/10.1002/1521-3765(20010216)7:4<796::AID-CHEM796>3.0.CO;2-J).
- 29 R. Wang, L. Guo, H. Jin, L. Lu, L. Yi, D. Zhang and J. Chen, DFT Study of the Enhancement on Hydrogen Production by Alkaline Catalyzed Water Gas Shift Reaction in Supercritical Water, *Int. J. Hydrogen Energy*, 2018, **43** (30), 13879–13886, DOI: [10.1016/j.ijhydene.2017.12.075](https://doi.org/10.1016/j.ijhydene.2017.12.075).
- 30 T. Oldham, S. Yatom and E. Thimsen, Plasma Parameters and the Reduction Potential at a Plasma-Liquid Interface, *Phys. Chem. Chem. Phys.*, 2022, **24**, 14257–14268, DOI: [10.1039/D2CP00203E](https://doi.org/10.1039/D2CP00203E).
- 31 C. Willis and C. Devillers, The Pulse Radiolysis of Carbon Monoxide, *Chem. Phys. Lett.*, 1968, **2**(1), 51–53, DOI: [10.1016/0009-2614\(68\)80146-0](https://doi.org/10.1016/0009-2614(68)80146-0).
- 32 A. Fojtik, G. Czapski, A. Henglein and L. G. Czapski, Pulse Radiolytic Investigation of the Carboxyl Radical in Aqueous Solution, *J. Phys. Chem.*, 1970, **74**(17), 3204–3208, DOI: [10.1021/j100711a008](https://doi.org/10.1021/j100711a008).
- 33 Y. Gorbanev, D. O'Connell and V. Chechik, Non-Thermal Plasma in Contact with Water: The Origin of Species, *Chem. – Eur. J.*, 2016, **22**(10), 3496–3505, DOI: [10.1002/chem.201503771](https://doi.org/10.1002/chem.201503771).
- 34 E. Schuler, M. Morana, N. R. Shiju and G. J. M. Gruter, A New Way to Make Oxalic Acid from CO<sub>2</sub> and Alkali Formates: Using the Active Carbonite Intermediate, *Sustainable Chem. Clim. Action*, 2022, **1**, 100001, DOI: [10.1016/j.scca.2022.100001](https://doi.org/10.1016/j.scca.2022.100001).
- 35 I. Janik and G. N. R. Tripathi, The Nature of the CO<sub>2</sub>-Radical Anion in Water, *J. Chem. Phys.*, 2016, **144**(15), 154307, DOI: [10.1063/1.4946868](https://doi.org/10.1063/1.4946868).
- 36 G. V. Buxton and R. M. Sellers, Acid Dissociation Constant of the Carboxyl Radical. Pulse Radiolysis Studies of Aqueous Solutions of Formic Acid and Sodium Formate, *J. Chem. Soc., Faraday Trans. 1*, 1973, **69**, 555–559, DOI: [10.1039/F19736900555](https://doi.org/10.1039/F19736900555).
- 37 A. S. Jeevarajan, I. Carmichael and R. W. Fessenden, ESR Measurement of the pK<sub>a</sub> of Carboxyl Radical and Ab Initio Calculation of the Carbon-13 Hyperfine Constant, *J. Phys. Chem.*, 1990, **94**(4), 1372–1376, DOI: [10.1021/j100367a033](https://doi.org/10.1021/j100367a033).
- 38 U. Schuchardt, M. Fatima and B. Sousa, Oxalate as an Intermediate in the Base-Catalysed Water-Gas Shift Reaction, *Fuel*, 1986, **65**, 669–672, DOI: [10.1016/0016-2361\(86\)90362-5](https://doi.org/10.1016/0016-2361(86)90362-5).
- 39 D. C. Elliott and L. J. Sealock Jr, Aqueous Catalyst Systems for the Water-Gas Shift Reaction. 1. Comparative Catalyst Studies, *Ind. Eng. Chem. Prod. Res. Dev.*, 1983, **22**(3), 426–431, DOI: [10.1021/i300011a008](https://doi.org/10.1021/i300011a008).
- 40 D. C. Elliott, R. T. Hallen and L. J. Sealock Jr, Aqueous Catalyst Systems for the Water-Gas Shift Reaction. 2. Mechanism of Basic Catalysis, *Ind. Eng. Chem. Prod. Res. Dev.*, 1983, **22**(3), 431–435, DOI: [10.1021/i300011a009](https://doi.org/10.1021/i300011a009).

